

Observing Traveling Ionospheric Disturbances Caused by Tsunamis Using GPS TEC Measurements

David A. Galvan, *Caltech/JPL*

, *Caltech/JPL*

Michael Hickey, *Embry Riddle Aeronautical University*

James Foster, *University of Hawaii at Manoa*

Anthony J. Mannucci, *Caltech/JPL*

BIOGRAPHY

David A. Galvan is a Caltech Postdoctoral Researcher at the Jet Propulsion Laboratory. He has studied magnetospheric and ionospheric physics, especially the density structure and dynamics of the Earth's plasmasphere. He is interested in coupling mechanisms between the ocean, atmosphere, ionosphere and magnetosphere. He earned his Ph.D. in Geophysics and Space Physics from UCLA in 2009.

Attila Komjathy is a senior member of the Ionospheric and Atmospheric Remote Sensing (IARS) group of the Tracking Systems and Applications Section at NASA's Jet Propulsion Laboratory (JPL), California Institute of Technology. He specializes in various aspects of remote sensing techniques. He received his Ph.D. from the Department of Geodesy and Geomatics Engineering of the University of New Brunswick, Canada in 1997. Prior to joining JPL in 2001, he worked as a postdoctoral researcher at the University of Colorado at Boulder specializing in new GPS remote sensing applications.

Michael Hickey is a Professor at Embry Riddle Aeronautical University. He has recently developed a Spectral Full Wave Model to study coupling between the ocean surface, the atmosphere, and the ionosphere.

James Foster is an Assistant Researcher at the University of Hawaii at Manoa. His interests include Geodesy,

GPS meteorology and the impact and mitigation of the atmosphere on space geodetic measurements.

Anthony J. Mannucci is supervisor of the Ionospheric and Atmospheric Remote Sensing Group at NASA's Jet Propulsion Laboratory, where he has been working since 1989. Dr. Mannucci is an expert in the application of GPS signals to scientific investigations of the ionosphere and atmosphere, and has developed ionospheric calibration systems for deep space tracking and Earth science applications. He has pioneered the development of widely-used data analysis methods for calibrating GPS ionospheric measurements and for mapping ionospheric total electron content on regional and global scales. He obtained his Ph.D. in Physics from U.C. Berkeley in 1989.

ABSTRACT

Ground-based Global Positioning System (GPS) measurements of ionospheric Total Electron Content (TEC) show variations consistent with atmospheric internal gravity waves caused by ocean tsunamis following two recent seismic events: the American Samoa earthquake of September 29, 2009, and the Chile earthquake of February 27, 2010. Fluctuations in TEC correlated in time, space, and wave properties with these tsunamis were observed in TEC estimates processed using JPL's Global Ionospheric Mapping Software. These TEC estimates were band-pass filtered to remove ionospheric

TEC variations with wavelengths and periods outside the typical range of internal gravity waves caused by tsunamis. Observable variations in TEC appear correlated with the tsunamis in certain locations, but not in others. Where variations are observed, the typical amplitude tends to be on the order of 1% of the background TEC value. Variations with amplitudes $\sim 0.1 - 0.2$ TECU are observable with periods and timing affiliated with the tsunami. These observations are compared to estimates of expected tsunami-driven TEC variations produced by Embry Riddle Aeronautical University's Spectral Full Wave Model, an atmosphere-ionosphere coupling model, and found to be in good agreement in some locations, though there are cases when the model predicts an observable tsunami-driven signature and none is observed. These TEC variations are not always seen when a tsunami is present, but in these two events the regions where a strong ocean tsunami was observed did coincide with clear TEC observations, while a lack of clear TEC observations coincided with smaller tsunami amplitudes. There exists the potential to apply these detection techniques to real-time GPS TEC data, providing estimates of tsunami speed and amplitude that may be useful for early warning systems.

INTRODUCTION

The tsunami of September 29, 2009 caused an estimated 192 deaths (e.g., TV New Zealand, 2009; NOAA NGDC Event Summary, 2009) on the islands of Samoa, American Samoa, and Apia; and estimates for casualties from the Chilean tsunami of February 27, 2010 have ranged from 124 to 231 [e.g., Tang *et al.*, 2010; NOAA NGDC Event Summary, 2010, respectively]. Both tsunamis had a major impact on public consciousness as the $\sim 12 - 24$ hour time period between the earthquakes and the arrival of the tsunamis at Hawaii and communities on the Pacific Rim, such as Japan and the U.S. West Coast, caused much anxiety and coverage on the major news networks. There is a need for effective and reliable modeling and observational systems that can provide estimates of tsunami properties before the tsunami itself arrives at a given shore. Recent modeling results have demonstrated that the ionospheric signature of an ocean tsunami can potentially be detected as a traveling ionospheric disturbance (TID) produced by internal gravity waves propagating upward in the atmosphere [e.g., Occhipinti *et al.*, (2006, 2008), Hickey *et al.*, (2009), Mai and Kiang 2009]. These tsunami-driven TIDs have been demonstrated to be present in ionospheric total electron content (TEC) measurements using ground-based GPS radio signals [e.g., Artru *et al.*, (2005)].

Hines [1972] developed a theory of atmospheric gravity waves, mentioning the possibility that ocean tsunamis, in

addition to other terrestrial and atmospheric events like earthquakes and tropospheric storms, might generate internal gravity waves that could propagate to altitudes greater than 70 km. Peltier and Hines [1976] then demonstrated mathematically that the variations in ionospheric electron densities caused by these tsunami-driven internal gravity waves should be detectable in ionosonde measurements. The only gravity waves capable of propagating to ionospheric heights are those that oscillate below the Brunt Väisälä frequency (ω_b), the natural buoyancy frequency at which a parcel of air will oscillate when displaced from its equilibrium position [e.g., Kelley, 2009]. Essentially, a parcel of air that is displaced upward in the atmosphere will find itself surrounded by air that is less dense than itself, and will fall back downward until it is surrounded by air that is more dense, at which point it will be buoyed upward again, oscillating about the equilibrium height at a frequency of ω_b . In the Earth's atmosphere, ω_b ranges from 3.3 to 1.1 mHz depending on altitude, corresponding to a buoyancy period ~ 5 min at sea level, and ~ 15 minutes at 400 km altitude, near the F-region peak of the ionosphere [Yeh and Liu, 1974]. Tsunamis can have periods ranging from 5 minutes up to an hour, but the typical deep ocean period is 10 – 30 minutes. Thus a tsunami may induce an internal gravity wave that reaches the ionosphere even though the tsunami amplitude in the deep ocean is only a few centimeters. In contrast, the typical background noise of ~ 1 m amplitude ocean surface waves, with periods of several to tens of seconds, produce only evanescent waves in the atmosphere, with amplitudes decreasing exponentially with altitude [e.g., Hines, 1972], and hence this background ocean surface activity does not affect measurements of TEC by GPS.

There have been several studies observing variations in ionospheric electron density associated with ocean tsunamis. These observations have typically been made using line-of-sight integrated electron density, or total electron content (TEC), measurements available from satellite-carried nadir-looking radar altimeters (e.g., on the TOPEX/Poseidon and Jason satellites), or time delay of radio signals sent from GPS satellites to ground-based receivers. Artru *et al.*, [2005] showed variations in TEC as observed by over 1000 receivers in the Japanese GEONET network coincident with the arrival at Japan of a tsunami generated by an earthquake in Chile. Occhipinti *et al.*, [2006] and Mai and Kiang [2009] showed perturbations in the TEC derived from the Jason-1 radar altimeter after the 2004 Sumatra tsunami. Such observations have offered hope that the ionospheric signature of ocean tsunamis can indeed be remotely observed, however there are other sources for TIDs not associated with tsunamis, such as intense tropospheric weather [Hung *et al.*, 1978, Kelley 1997; Xiao *et al.*, 2006], geomagnetic and auroral activity [Richmond and Matsushita, 1975; Nicolls *et al.*, 2004], and earthquakes

[*Calais and Minster, 1995; Artru et al., 2001; Kelley et al., 1985*]. The existence of non-tsunami-driven TIDs may make detection and confirmation of tsunami association more challenging [e.g., *Artru et al., 2005*]. In our current research, we distinguish ionospheric signatures of tsunami-driven TID's by verifying that the horizontal speed and direction of the TID match that of the ocean tsunami.

In addition to observations, progress has been made in the theoretical modeling of the interaction between the ocean surface, atmosphere, and ionosphere. *Occhipinti et al., [2006]* demonstrated a three-dimensional model predicting the variation in TEC that should be observed from a given ocean tsunami amplitude and period. *Occhipinti et al., [2008]* then showed that the neutral-plasma coupling involved in transferring the wave energy from the atmosphere to the ionosphere varies with the orientation of the Earth's magnetic field, leading to more efficient coupling at lower rather than higher geomagnetic latitudes. *Hickey et al., [2009]* improved on the gravity wave modeling by including the effects of wave damping via thermal conduction, ion drag, and molecular viscosity, as well as the filtering effects of background atmospheric winds. These recent modeling results have shown, for instance, that strong zonal winds in the low-latitude upper atmosphere may make the variation in TEC produced by east-west propagating tsunamis far lower in magnitude than variations produced by north-south propagating tsunamis. Such geophysical subtleties affecting the ability of tsunami-driven internal gravity waves to perturb the ionosphere create additional challenges in developing a routine method of detection via GPS TEC.

In this paper, we discuss observation and model results from the Samoa tsunami of September 2009, and the Chile tsunami of February 2010. Using JPL's Global Ionospheric Mapping (GIM) software to remove hardware biases and extract TEC measurements from GPS receivers, we have analyzed GPS TEC data from these events in an effort to determine the consistency and nature of TEC variations associated with tsunamis. We compare our observations with estimates of predicted TEC variation magnitude from the *Hickey et al., [2009]* model for ocean-atmosphere-ionosphere coupling.

METHODOLOGY

Networks of GPS Receivers

Dual-frequency GPS receivers are capable of producing the time delay and phase advance observables that can be processed to produce TEC measurements. There are several major networks of ground-based, dual frequency GPS receivers that can be used to produce TEC observations. The International GPS Service (IGS) network, for example, is a global network of over 350

continuously operating dual-frequency GPS stations. This type of network provides widespread but sparse coverage; useful because, no matter where a tsunami occurs, there will likely be a GPS receiver in the vicinity that may be used to look for TEC variations. There are also major regional networks, such as Japan's GEONET network of over 1200 GPS stations, Southern California's Plate Boundary Observatory (PBO) network of over 875 stations, and the University of Hawaii's Pacific GPS Facility of dozens of receivers on the big island of Hawaii. These regional networks provide highly localized but very dense coverage, allowing for corroboration of observations via many GPS TEC observations in a particular region. We utilize all GPS stations available in a particular region of interest for our studies, sometimes using stations from multiple overlapping networks.

GIM Processing

For these studies, we use the Global Ionospheric Mapping (GIM) (e.g., *Komjathy et al., 2005; Mannucci et al., 1998*) software suite to process the Receiver Independent Exchange format (RINEX) files from networks of GPS receivers in order to produce TEC values between the ground receivers and GPS satellites. GIM was developed to compute high-precision ionospheric delay measurements by estimating and subsequently subtracting the satellite and receiver differential biases from the ionospheric observables. Overall accuracy for absolute TEC values tends to be +/- 1-2 TECU. However, for our study we are interested in monitoring small-scale variations in ionospheric electron density, hence changes in TEC are our data set of interest, rather than absolute TEC values. The precision uncertainty for variations in TEC measurements using the GIM processing is typically about +/- 0.1 TECU.

Slant TEC Analysis

After selecting the stations of interest based on the geographic domain of a given tsunami, we process the GPS RINEX files using the GIM software. We then produce slant-TEC time series for the stations of interest in the time period when the first wave front of the tsunami should be moving through the vicinity of the receivers. Our current technique is a method for analyzing historical tsunami events to determine whether these tsunamis produced a detectable variation in ionospheric electron density. In the future, we hope to develop algorithms that will begin monitoring particular real-time GPS receiver observations in regions based on the epicenter location of the seismic source of the tsunami.

Ocean tsunamis tend to have wave periods ranging between 5 minutes and 1 hour, depending on the ocean depth, with typical deep ocean periods around 30 minutes, wavelengths ~400 km, and speeds of ~200 m/s [e.g., *Peltier and Hines, 1976*]. In order to remove longer

period variations in TEC time series (such as diurnal variations and multiple-hour trends due to changing elevation angle of the receiver-satellite line-of-sight), we use a zero-phase bi-directional band-pass filter with a pass band of 0.5 to 5 mHz (corresponding to wave periods of 2000 to 200 seconds; 33.3 minutes to 3.3 minutes) to extract variations in TEC with periods similar to that of the ocean tsunami itself. Figure 1 shows an example of this analysis technique applied to the TEC time series from the Anipeahi (ANIP) GPS receiver on the big island of Hawaii about 6.5 hours after the earthquake on September 29, 2009.

The upper plot displays the absolute slant TEC (STEC) values observed in the line-of-sight between the ANIP receiver and the SVN 40 GPS satellite, with a 10th order polynomial curve fit to the measurements. The middle panel shows the residual differences between the polynomial fit and the actual observations. The bottom plot indicates the variations in the absolute TEC after running the data through the band-pass filter. By applying this filtration process on the GIM-processed

to more effectively search for variations in TEC that may be associated with tsunamis. Note the variations in TEC clearly visible in all three plots, ranging from ~23:55 on September 29 to 00:50 UT on September 30. Note the variation has a period of approximately 27 minutes, similar to the ocean surface tsunami period of approximately 30 minutes observed by various tidal gauges throughout the Hawaiian islands [NOAA Center for Tsunami Research Event Page: Samoa 2009]. Similar variations during this time period (not shown) are evident in STEC time series from many other Hawaiian GPS receivers in communication with both the SVN 40 and SVN 50 GPS satellites. The perturbation to background TEC is quite distinct, but in order to determine whether it is caused by a tsunami, the earthquake itself, or some other phenomenon, we must analyze the data further to determine the horizontal speed of the traveling disturbance. This analysis requires an understanding of the phenomenology behind atmospheric wave propagation.

The F-region of the ionosphere, centered at 350-400 km

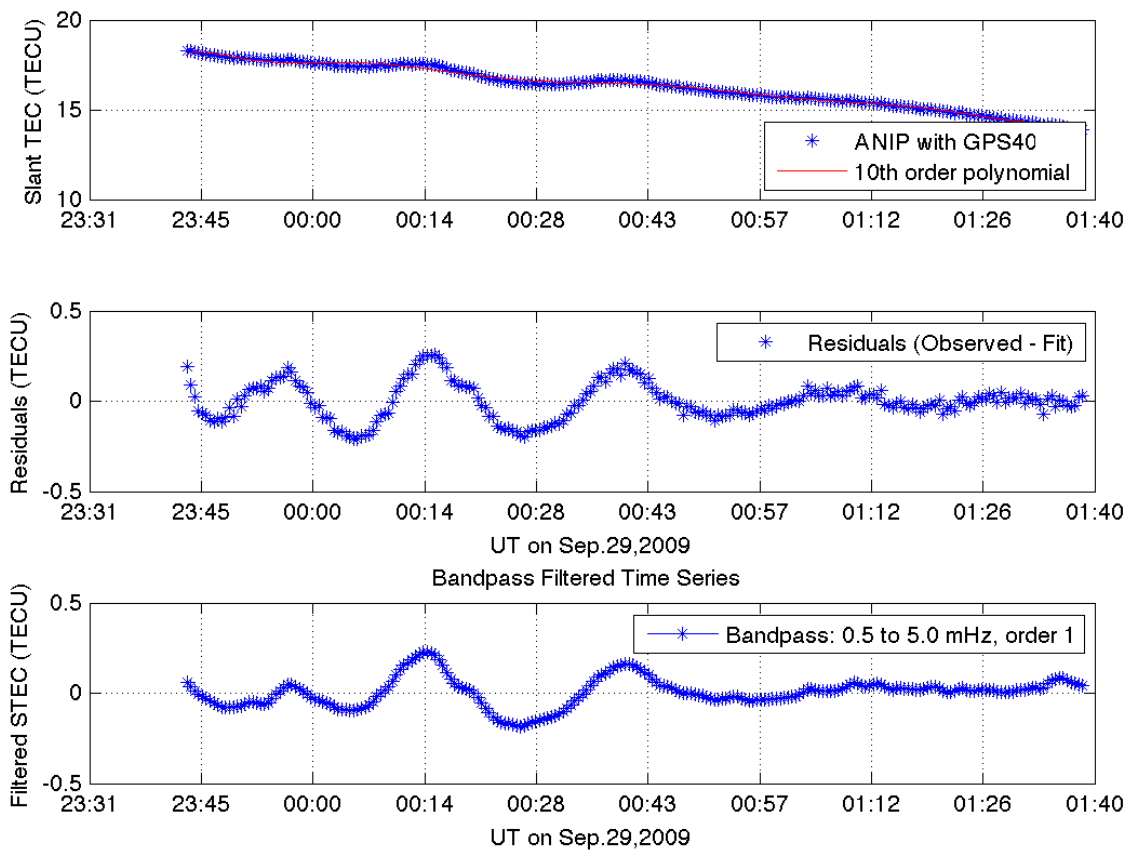


Figure 1. Time series observations of STEC (top), residuals with a fit to a high-order polynomial (middle), and band-pass filtered STEC (bottom) for the Anipeahi (ANIP) GPS receiver on Hawaii in communication with GPS satellite SVN 40.

STEC data using all GPS receivers available, we are able

altitude, depending on local time and latitude, contains the

bulk of the free electrons in the ionosphere, and therefore makes the largest contribution to measurements of ionospheric TEC. Hence, any tsunami-driven atmospheric wave that could be visible as a variation in TEC would need to propagate from the ocean surface up to about 350–400 km altitude before TEC measurements could detect it. Different types of atmospheric waves have different propagation velocities. A typical acoustic wave, often generated by the earthquake itself, can propagate through the atmosphere at the sound speed, which varies from several hundred m/s near sea level to ~ 1 km/s at 400km altitude. It would take approximately 10 - 15 minutes for such a wave to affect the F-region, and thus TEC observations. The initial seismic source at the epicenter can generate an acoustic wave that propagates isotropically in the atmosphere, hence both vertical and horizontal propagation speeds would be the same (the sound speed of the atmosphere). By the time the wave reached the F-region, the horizontal velocity of the perturbation in TEC would be ~ 1 km/s. However, earthquakes also generate Rayleigh waves, transverse

solid-Earth waves that propagate along the surface, with a horizontal velocity of about 3.4 km/s. These solid-Earth waves, too, produce acoustic waves in the overlying atmosphere, and these acoustic waves propagate upward at the atmospheric sound speed ($\sim 300 - 1000$ m/s depending on altitude). As the wavefront of the Rayleigh wave moves horizontally along the land, new atmospheric acoustic waves are generated, such that the variation in electron density in the ionosphere would appear to be moving horizontally at 3.4 km/s, following the solid-Earth wave [e.g., *Artru et al.*, 2001; *Hines*, 1972]. Such earthquake-generated waves have been detected in ionospheric TEC in the past [e.g., *Calais and Minster*, 1995; *Kelley et al.*, 1985]. Earthquake-generated ionospheric disturbances must be taken into account because they could be mistaken for tsunami-driven signals, but would exist regardless of whether a tsunami was generated, since not all submarine earthquakes produce tsunamis.

Acoustic waves may be considered sound waves resulting

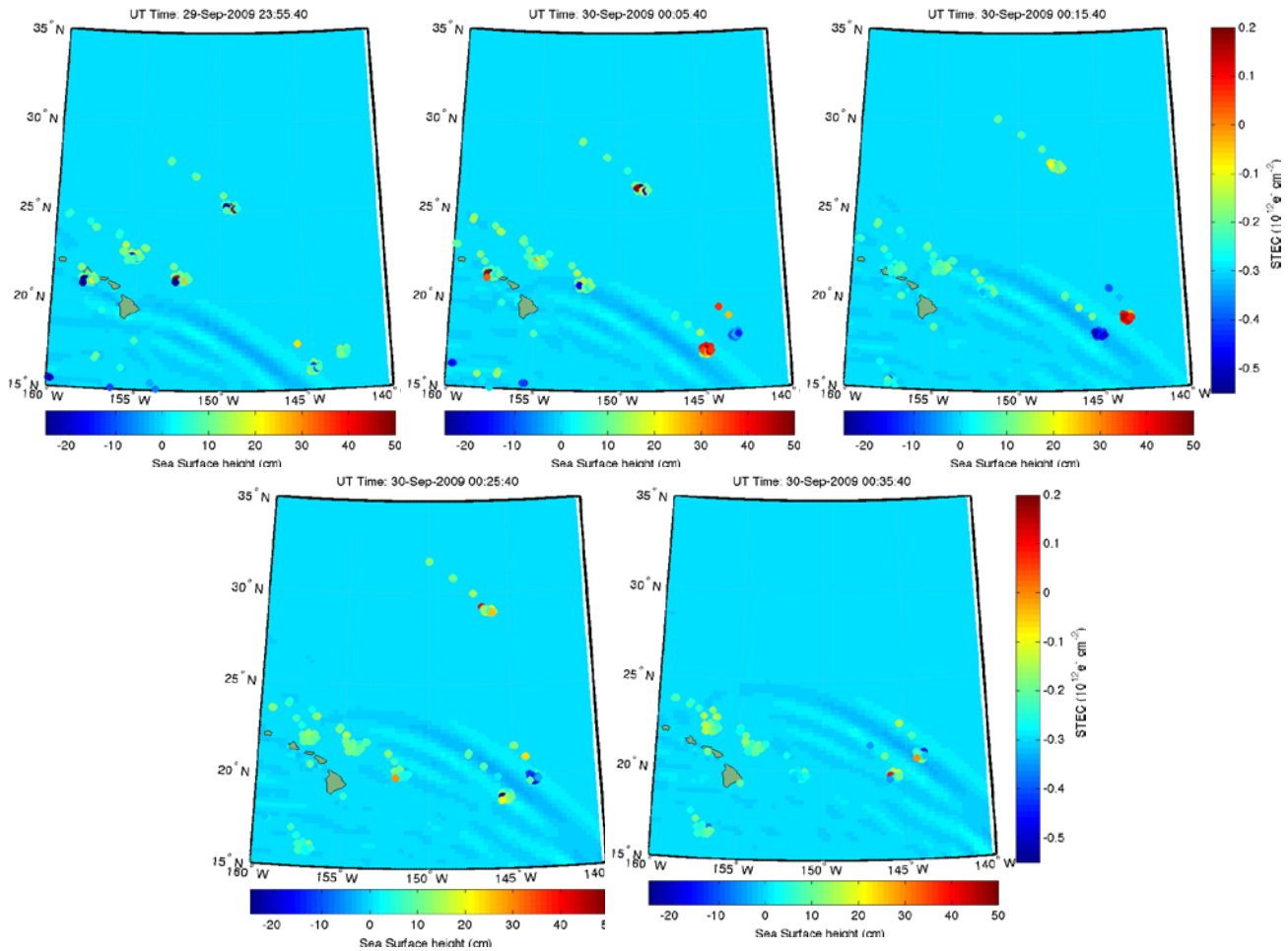


Figure 2. Band-pass filtered STEC plotted in color at ionospheric pierce point locations for 76 GPS receivers on the Hawaiian Islands, plotted every 10 minutes from 22:55:40 on 29-September through 00:35:40 on 30-September, 2009. Tsunami sea surface heights estimated by the MOST model are overplotted to show correlation between variations in STEC and passage of the tsunami.

from longitudinal compression in the direction of propagation. Internal gravity waves, on the other hand, are buoyancy waves resulting from vertical transverse oscillations of parcels of air caused by a slow rise and fall of the Earth's surface; in this case the ocean. With vertical propagation velocities on the order of 40 m/s [Artru *et al.*, 2005], these waves are expected to reach the F-region in over 2 hours. The horizontal velocity of observed perturbations will match the horizontal velocity of the tsunami itself ~ 200 m/s. Thus, one way to distinguish signals associated with a tsunami is to look for coherent TEC variations, observed by multiple satellites and receivers, that are propagating at ~ 200 m/s in an outward direction from the tsunami's source. We employed this method of first finding a TEC variation of the appropriate amplitude, and then plotting the TEC values as a function of distance and time to see if the variation is aligned with a gravity wave horizontal velocity.

COMPARISON WITH MODEL RESULTS AND BUOY OBSERVATIONS

We use the Hickey *et al.*, [2009] spectral full-wave model

(SFWM) to produce an estimate of the expected perturbation to ionospheric TEC resulting from the known ocean tsunami amplitude, period, and azimuthal direction. The SFWM numerically simulates the upward propagation of a spectrum of gravity waves in the atmosphere, and the interaction of those gravity waves with the ionosphere in the F-region, where the electron density of the ionosphere peaks and therefore the greatest contribution to line-of-sight TEC is made. The model assumes a non-isothermal atmosphere, and takes into account such subtleties as eddy and molecular diffusion of heat and momentum, as well as ion drag, Coriolis force, and the altitude-variation of mean winds in the atmosphere.

To produce the initial perturbation of the lower boundary of the modeled atmosphere, we use sea surface height amplitudes associated with the tsunami at a given location. The sea surface height is obtained from one of two sources: the modeled height estimated by the Method of Splitting Tsunami (MOST) model produced by the NOAA Center for Tsunami Research (e.g., Titov *et al.*, 2005; Titov and Gonzalez, 1997; Titov and Synolakis, 1997), or the measurements made by various tidal gauges

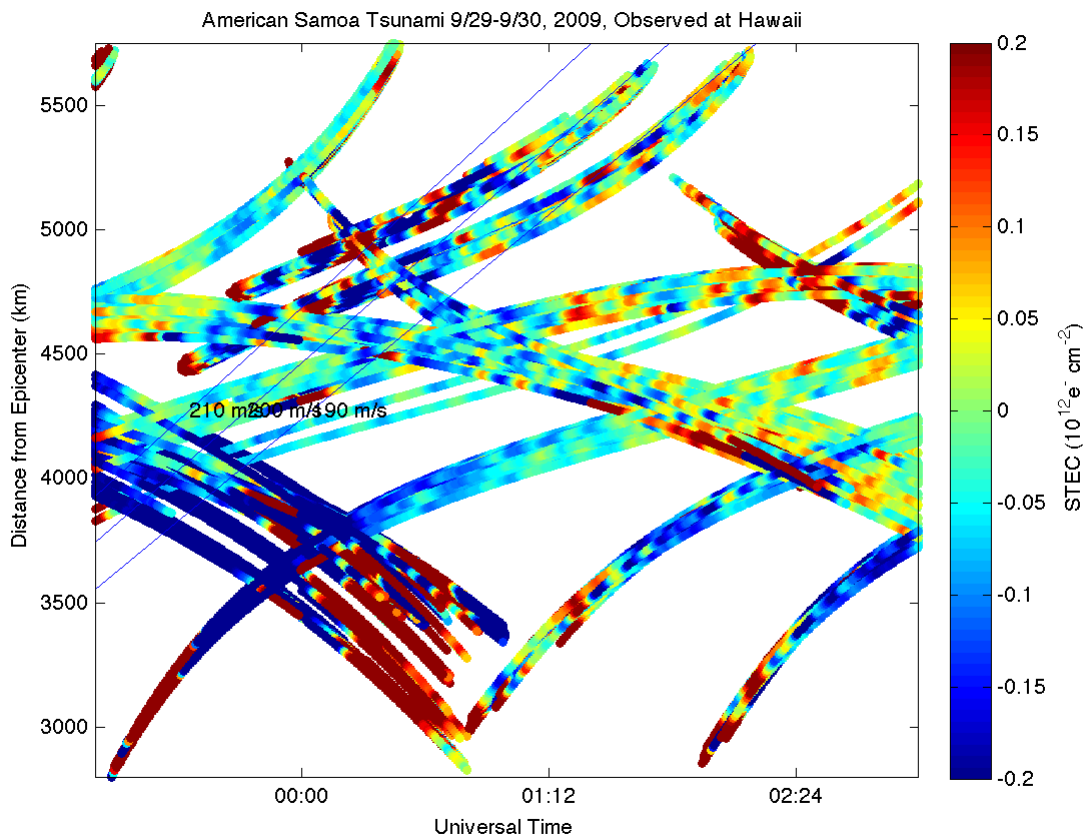


Figure 3. Distance from epicenter vs. time plot showing band-pass-filtered STEC for 76 GPS receivers on the Hawaiian Islands at the time the tsunami passed by the islands. Overplotted lines show the expected alignment of variations traveling at internal gravity wave speeds ~ 200 m/s.

and ocean buoys around the world, such as the Deep-ocean Assessment and Reporting of Tsunamis (DART) buoy system throughout the Pacific ocean (e.g., *Meinig et al.*, 2005). This sea surface tsunami waveform (whether it is observed in buoy data or a result of the MOST model) is used as an input for the *Hickey et al.* [2009] model, which then determines the expected variation in ionospheric TEC due to the ocean surface perturbation.

RESULTS

American Samoa Tsunami of September 29, 2009

At 17:48:11 UT on September 29, 2009, a magnitude 8.1 Earthquake struck at 15.5 south latitude, 172.0 west longitude, 195 km south of Apia, Samoa. The earthquake produced a tsunami that arrived at the city of Pago Pago on American Samoa at 18:12 UT, according to near-shore tidal gauges, causing significant damage. Figure 1 shows STEC measurements from the Anipeahi (ANIP) GPS receiver on the big island of Hawaii, as previously described. These ionospheric variations take place at about the same time the tsunami is observed to

pass by the Hawaiian Islands, having travelled from the earthquake epicenter near American Samoa for about 6.5 hours, allowing plenty of time for the atmospheric gravity wave to reach the ionosphere and thus become detectable to GPS TEC measurements. Note that both the residuals (middle plot: the difference between the observed STEC and a 10th order polynomial fit) and the band-pass filtered STEC (bottom plot) show significant variations with amplitudes up to ~0.3 TECU (1 TECU = 10¹⁶ e/m²).

Figure 2 shows a series of instantaneous maps of the region surrounding the Hawaiian Islands, with band-pass filtered STEC plotted in color from 76 GPS receivers on Hawaii, mostly on the big island. The variations in STEC are plotted at the geographical locations of the ionospheric pierce points (IPPs), the geographic positions at which the line-of-sight between the GPS receiver on the ground and the GPS satellites in orbit penetrate the F-region at the ionospheric shell-height (selected to be 400 km in our case), where the variation in TEC is expected to be the most significant. In addition, sea-surface height amplitudes generated by the MOST model are overplotted to show the estimated location of the tsunami wave fronts

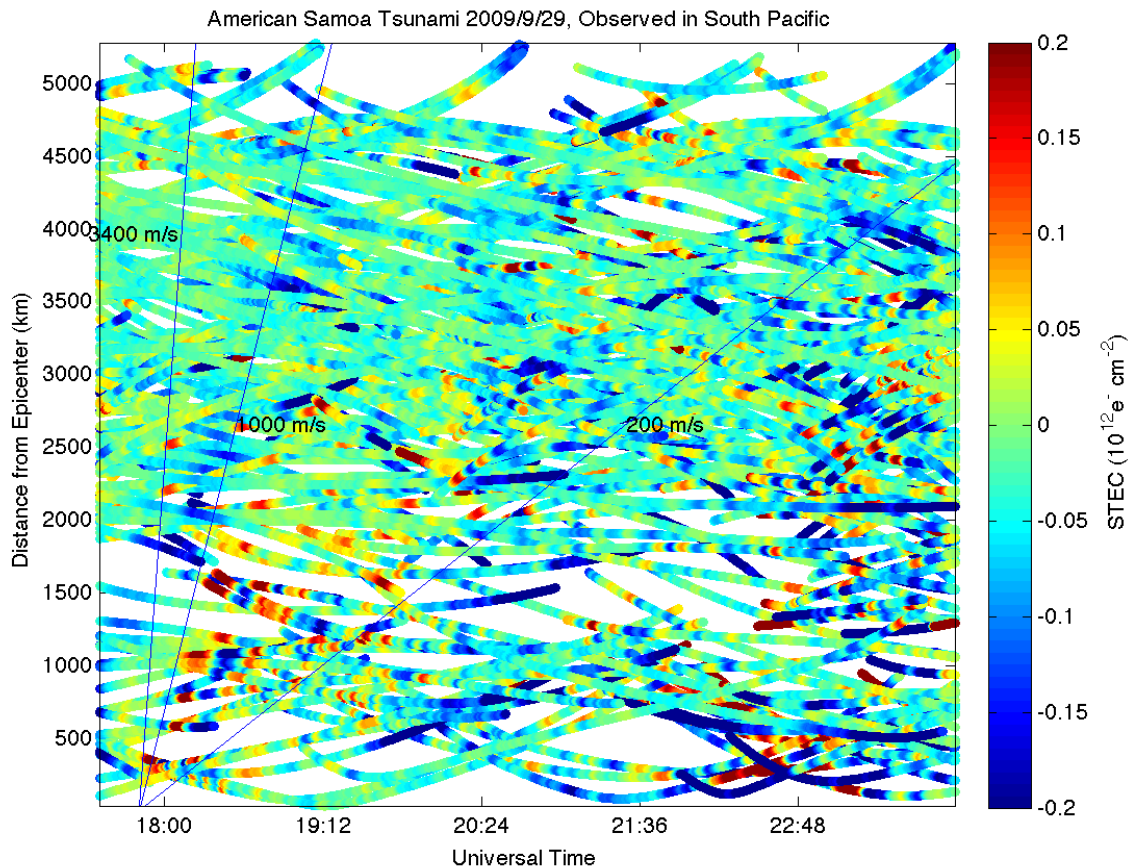


Figure 4. Distance from epicenter vs. time plot showing band-pass-filtered STEC for IGS GPS receivers on the Hawaiian Islands at the time the tsunami passed by the islands. Overplotted lines show the expected alignment of variations from atmospheric gravity waves (200 m/s), acoustic waves (1000 m/s) and Rayleigh waves (3400 m/s).

for this event. Note that, just as the MOST model wave fronts are moving past the southeastern IPPs, the STEC variation in that region becomes quite pronounced, correlated with the passage of the ocean tsunami itself.

Fig. 3 shows a distance vs. time plot of the STEC observations from the 76 Hawaiian GPS receivers in the Pacific GPS Facility network on a distance vs. time “hodochron” plot. Band-pass filtered STEC values are shown in color as a function of distance between the ionospheric pierce points and the epicenter (ordinate) and time since the earthquake (abscissa). This type of distance vs. time (or “hodochron”) plot is useful because a constant speed can be represented as a straight line, the slope of which is the velocity magnitude. The variation is seen in the upper left of the plot as a low-high-low variation with amplitudes of 0.2 TEC units. The overplotted velocity lines show that these variations are consistent with what we would expect to see from an

internal gravity wave traveling with a horizontal wave velocity near 200 m/s coming from the epicenter of the American Samoa tsunami.

Note that tsunami-driven internal gravity waves were not seen in every region that encountered the tsunami itself, most notably the region near the Samoa earthquake epicenter. Fig. 4 shows another hodochron plot, displaying band-pass filtered STEC in the region near the epicenter of the Samoa earthquake, plotted as a function of distance from the epicenter and universal time. We overplot several lines representing constant horizontal velocities: one for Rayleigh wave speed at 3.4 km/s, one for acoustic waves traveling at 1000 m/s, and one for tsunami-driven gravity waves traveling near 200 m/s. Note there is a strong variation observed within 2000 km of the epicenter, and moving at a horizontal velocity \sim 1000 m/s, implying that the variations observed near the epicenter were traveling horizontally in the ionosphere at the speed of sound. This means the disturbance was

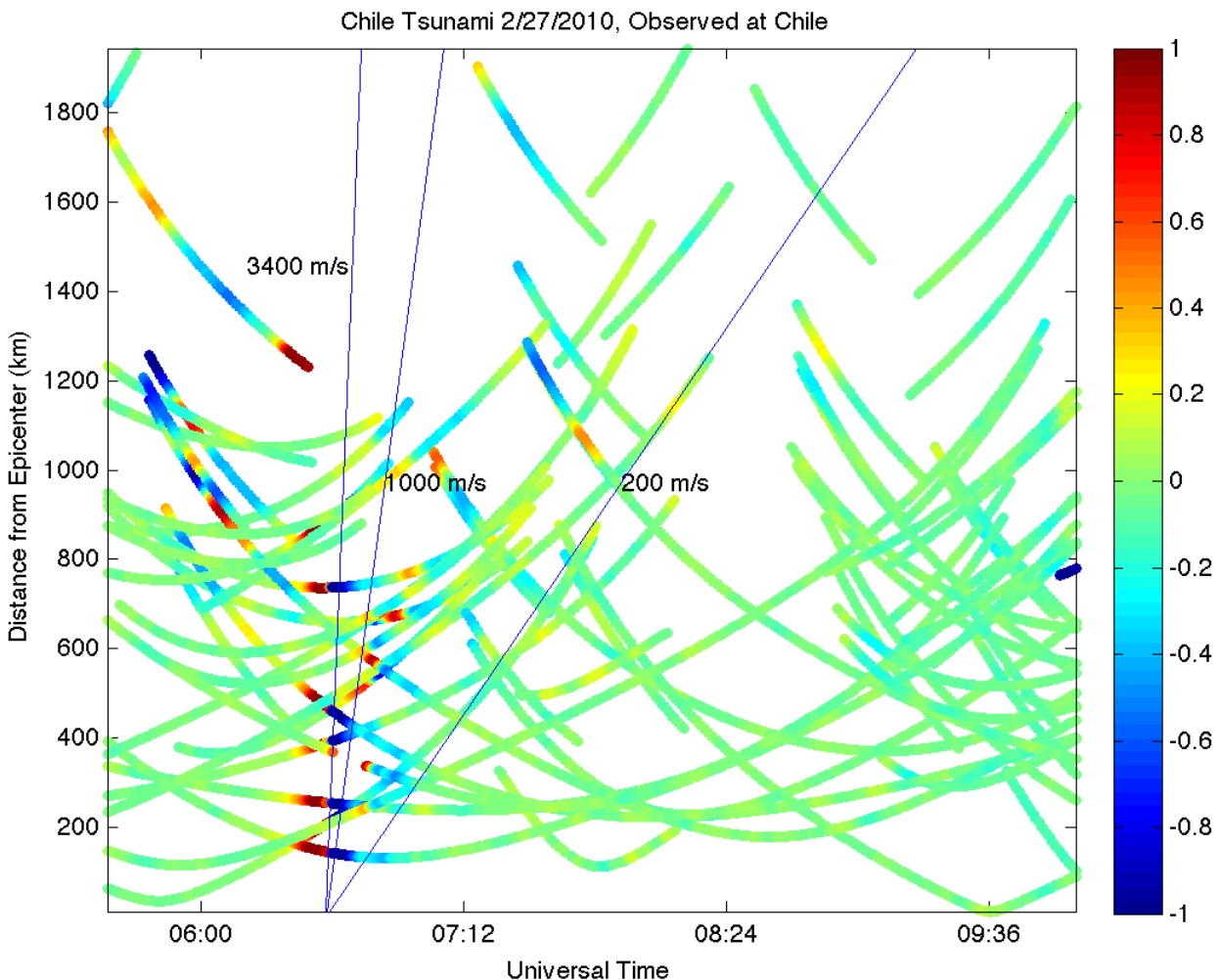


Figure 5 Slant TEC variation (shown in color) at Ionospheric Pierce Points at an altitude of 400 km, plotted as a function of distance from the epicenter of the Chile earthquake of February, 2010, and Universal time. Lines show horizontal velocities of gravity waves (200 m/s), acoustic waves (1000 m/s) and Rayleigh waves (3400 m/s).

likely caused by acoustic waves, not gravity waves, and is likely due to the earthquake itself, not the tsunami. Internal gravity waves generated by the tsunami would likely travel horizontally in the atmosphere around the same speed as the tsunami itself, ~ 200 m/s. No TEC variations aligned near the 200 m/s line are visible near the epicenter.

Interestingly, though tidal gauges along the coast of California show tsunami amplitudes ~ 10 cm close to shore from this event, no ionospheric TIDs were observed to accompany the ocean tsunami in the ionosphere over California. One possible explanation for this absence of observation may be that the tsunami was too weak to generate a significant internal gravity wave by the time it reached the U.S. west coast. This may be understandable, as the energy of a given section of the tsunami should decrease as the waves expand farther outward from the epicenter. The two DART buoys stationed off the California coast (station 46412, 190 NM West-Southwest of San Diego; and station 46411 stationed 260 NM Northwest of San Francisco) detected no significant tsunami, and were not triggered to enter their “event mode” of higher time-resolution data

logging. The next closest DART buoys to observe the tsunami, station 46404, 230 NM west of Astoria, Oregon, and station 46407 210 NM west of Cocos Bay, Oregon, detected a sea-surface height variation with amplitude < 2 cm. This is less than half the amplitude of the tsunami when it was observed near the epicenter at DART stations 51425 and 51426. All other DART buoys along the west coast of North America and the Aleutian islands detected sea surface variations of < 1 cm.

Chile Tsunami of February 27, 2010

The Chile event of February 27, 2010 provides an additional opportunity to search for tsunami-driven internal gravity waves using GPS receivers, as the ocean waves were detected in tidal gauges and buoys throughout the Pacific basin. This tsunami was generated by a magnitude 8.8 earthquake which occurred at 06:34 UT about 115 km Northeast of the coastal town of Concepcion, Chile. We analyzed TEC data from the dense network of GPS receivers in Hawaii and Southern California in order to observe the variation in TEC caused by tsunami-driven internal gravity waves traveling

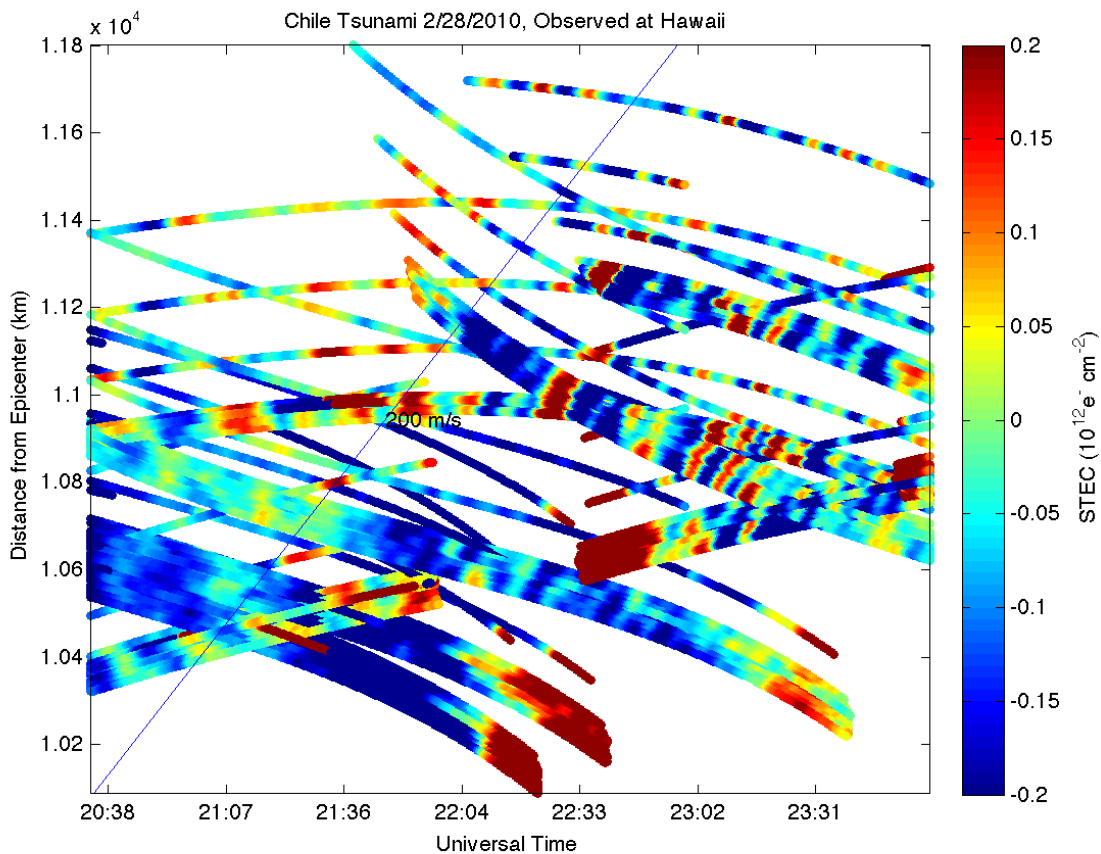


Figure 6. Band-pass filtered slant TEC variation (shown in color) at ionospheric pierce points at an altitude of 400 km, plotted as a function of distance from the epicenter of the Chile earthquake of February, 2010, and Universal time. Line shows a horizontal velocity of 200 m/s, corresponding to atmospheric gravity waves.6

through the ionosphere.

There are few GPS receivers from the IGS network along the South American west coast. We used 6 IGS receivers in to investigate the ionospheric behavior in the few hours immediately after the earthquake. Figure 5 shows a hodochron plot for the IPPs within 2000 km of the epicenter of the Chile earthquake. Again, velocity lines are plotted for tsunami-driven internal gravity waves, acoustic waves, and Rayleigh waves. There appear to be traveling ionospheric disturbances with horizontal velocities of ~ 1000 m/s, and ~ 3400 m/s, but no clear indication of a TID with a horizontal velocity near 200 m/s. There are few IPPs in the region where one would expect to first see a tsunami-driven TID, since the internal gravity wave would take ~ 2 hours to reach the ionosphere, putting the first detection possible at approximately 1500 km away from the epicenter. As such, we look farther afield for a tsunami-driven signature from this event.

The next region we investigate for this event is Hawaii. 62 GPS receivers on the Hawaiian islands had data available for TEC observations during the arrival of the tsunami. Figure 6 shows a hodochron plot for STEC

data from those receivers, with a 200 m/s horizontal velocity line overplotted. This plot only shows band-pass-filtered STEC variations for TEC raypaths with elevation angles greater than 30 degrees, in order to reduce the amount of low-elevation-angle data which tends to have greater noise. Note there are several clear TIDs that appear to be aligned parallel to the overplotted 200 m/s line. These variations could not be acoustic waves coming from the earthquake, for several reasons: first, any such acoustic waves traveling at a horizontal velocity near 1000 m/s would have long since passed Hawaii at this universal time; and second, TIDs associated with such acoustic waves would be aligned at a steeper slope corresponding to the 1000 m/s horizontal velocity, the line for which is not shown because it is out of the geographic bounds of this plot. Also note that there are several 200 m/s TIDs, each decreasing in intensity and period as time goes on, just as happens with an ocean tsunami.

We also processed TEC data from over 350 GPS receivers in the Southern California region for this event. Each of those GPS receivers was in line-of-sight with up to 12 GPS receivers at one time, resulting in several thousand sets of STEC time series. We ran the Hickey et

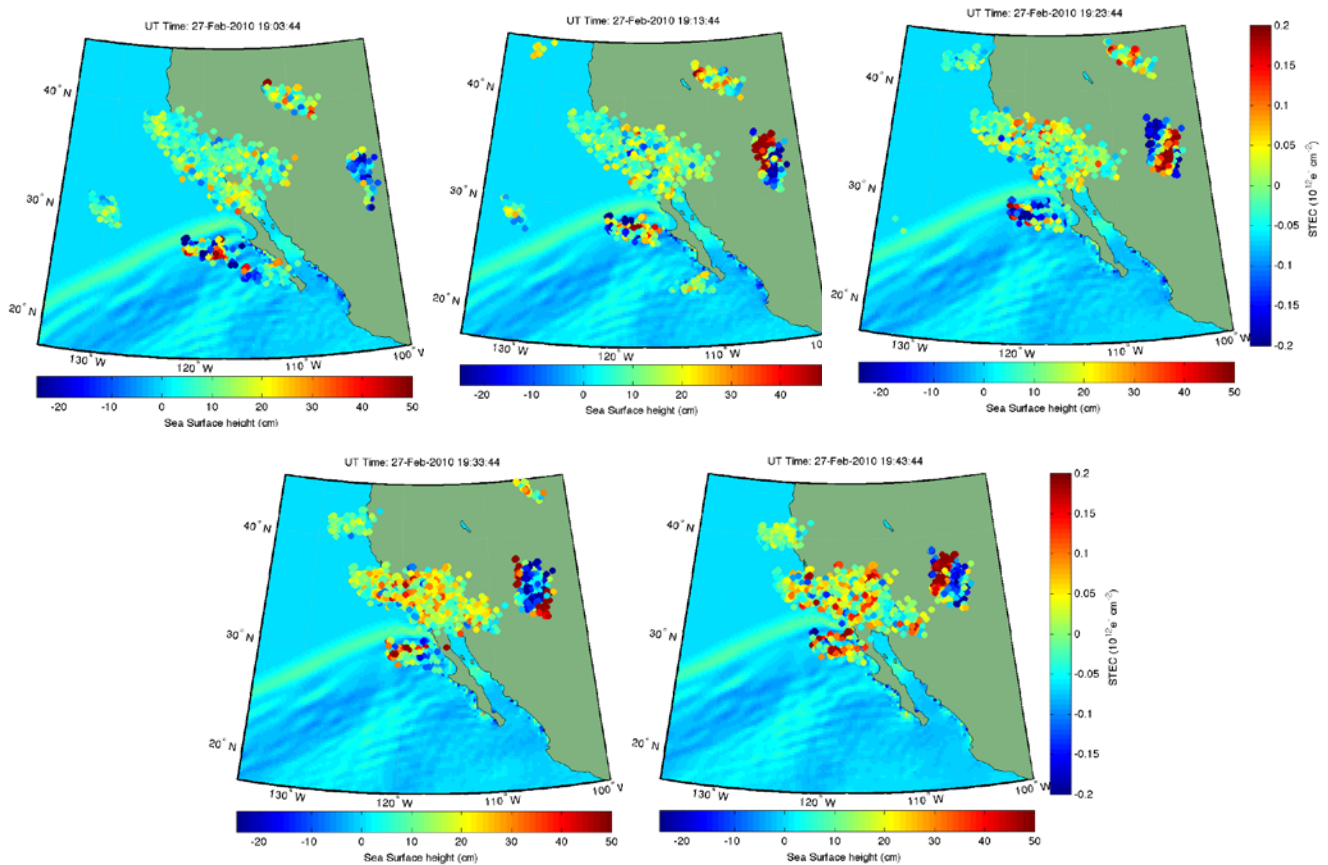


Figure 7. Band-pass filtered STEC plotted in color at ionospheric pierce point locations for 137 GPS receivers on the U.S. West Coast, plotted every 10 minutes from 19:03:44 through 19:43:44 on 27-February, 2010. Tsunami sea surface heights estimated by the MOST model are overplotted to show correlation between variations in STEC and passage of the tsunami.

al., 2009 spectral full wave model (SFWM) for this event, using as input the sea surface height observations from DART buoy # 46412, 190 nautical miles southwest of San Diego, CA. At this buoy, the tsunami had an amplitude of about 6 cm, with a period of approximately 24 minutes. The SFWM model predicts an ionospheric TEC variation of 2-2.5% of the background should occur based on this lower boundary input.

While this observation from an individual receiver may seem to corroborate the model's prediction, when we look at additional receivers we find that the observed TID is indeed significant, but that it appears to be propagating toward the southeast, while the tsunami is propagating toward the northwest. Fig. 7 shows a sequence of geographical maps showing the band-pass filtered variations in STEC at IPP locations, similar to Fig. 2, but for the region around California at the time when the Chile tsunami is passing through the region. Again, the MOST model sea surface heights are overplotted to show the location of the tsunami wavefronts at each time-stamped map. Note the significant wave-like TID visible by two satellites in the right-hand side of each figure panel. The disturbance is visible by most of the GPS receivers, and two of the GPS satellites, so is likely to be real, and it appears to be propagating toward the southeast. The variation in STEC has a period of about 28 minutes, and an amplitude of ~ 0.6 -1 TECU, with a background absolute TEC ranging from 27 – 31 TECU (for certain receivers). Thus the observed variation has a range of approximately 1.9 – 3.7% of the background TEC, in acceptable agreement with the model-predicted 2-2.5%, and the period is similar as well (~ 28 minutes in TEC vs. 24 minutes in the ocean). However, note that this variation is propagating toward the southeast, while the tsunami itself (and hence any gravity waves it generates) is propagating toward the northwest. This appears to be an example of a coincidental observation of a TID from another source, unrelated to the passing tsunami. This is a surprising result as the SFWM suggests that we should see an ionospheric signature of the tsunami in the region near southern California, and similar conditions produces a clear signature of the tsunami at Hawaii. This only emphasizes that care must be taken if applying this observation technique in a real-time operational manner: not all variations in ionospheric TEC can be attributed to the tsunami, even when they appear to be correlated with model results in amplitude and period. The direction and speed of propagation must match that of the tsunami itself.

Japan has over 1200 dual frequency GPS receivers in its GEONET network, making it an excellent region to search for ionospheric perturbations. Figure 8 shows a "hodochron" plot of band-pass filtered STEC (in color) as a function of distance and time in the ionosphere over

Japan at the time when the Chilean tsunami arrived in the region. Overplotted lines show velocities near the observed tsunami speed of ~ 200 m/s. There is a significant amount of noise in the data, however there appears to be a signal aligned with the appropriate velocity for the tsunami (approximately 200 m/s), and is visible in STEC observations from multiple satellites and multiple GPS stations in Japan. In fact, there appear to be at least two visible waves of perturbed electron density passing over Japan in succession at the time of the tsunami's arrival.

DISCUSSION

To summarize our results: For the Samoa event of 2009, we observed an ionospheric signature of a tsunami-driven internal gravity wave at Hawaii, but not near the epicenter or at the U.S. west coast. The lack of observation near the earthquake epicenter makes sense considering the ~ 2 hours it likely takes for the internal gravity wave to reach the F-region of the ionosphere at 400 km. The lack of observation in California may be explained by very low tsunami wave amplitudes in that region, generating an internal gravity wave that is below our TEC variation detection threshold of 0.1 TECU (precision uncertainty). For the Chile event of 2010, we observed what appears to be a tsunami-driven TID at Hawaii and at Japan, far afield from the source, but not near the epicenter and (surprisingly) not in California. The TEC observations at California deserve further attention, as we would expect to see a tsunami-driven internal gravity wave there, but instead see what appears to be a significant TID moving in the wrong direction, presumably from some source other than the tsunami.

Due to the geometry involved in TEC raypaths between GPS satellites and ground-based receivers, a disturbance in electron density moving through the ionosphere can be observed from many hundreds of km away (horizontally), allowing the GPS receiver to detect the tsunami-driven variation before the ocean tsunami itself arrives at the shore. Though the ability to make such observations using TEC will vary on a case by case basis, this demonstrates that future systems that monitor real-time TEC immediately after a major earthquake could contribute additional early information to an existing tsunami warning system such as that employed by the Pacific Tsunami Warning Center, which currently uses modeled tsunami propagation models and DART buoy and tidal gauge observations.

There are significant challenges remaining in the long-term effort to use TEC observations to improve tsunami warning systems. Simply observing TEC variations with amplitudes and periods predicted by an atmosphere-ionosphere coupling model does not prove that a given traveling ionospheric disturbance is associated with a tsunami. Data from multiple receivers in a given region must be analyzed as well to determine

the direction and timing of the observed traveling ionospheric disturbance, and whether the disturbance is consistently detected by multiple satellites. Care must also be taken when analyzing TEC data near the earthquake epicenter, as the earthquake may generate TEC variations that would exist regardless of whether a tsunami was generated or not. This is apparently the case for both the Samoa and Chile events, since we observed acoustic waves (and, in the case of Chile, Rayleigh waves) within about 1500 km of the earthquake epicenter. This result implies that the internal gravity wave from the tsunami may indeed take 2 hours or more to reach the F-region peak of the ionosphere (as predicted by *Peltier and Hines, 1976*), while the acoustic waves generated by the earthquake would reach the

likely to have been caused by the ocean waves, and those TIDs which are unrelated. Further research is required to provide an automated routine method of verifying, with many GPS receivers, an observed TEC signal's association with a tsunami.

Based on our results, it seems the best chances to observe TEC variations caused by a tsunami-driven internal gravity wave is to look in regions far afield from the epicenter (> 1500 km, assuming a vertical propagation velocity of 50 m/s for the internal gravity wave and a horizontal propagation velocity of 200 m/s for the tsunami). Any future augmented tsunami warning systems using the TEC observation technique would therefore be most useful for providing updated observations of tsunami amplitude, period, and velocity

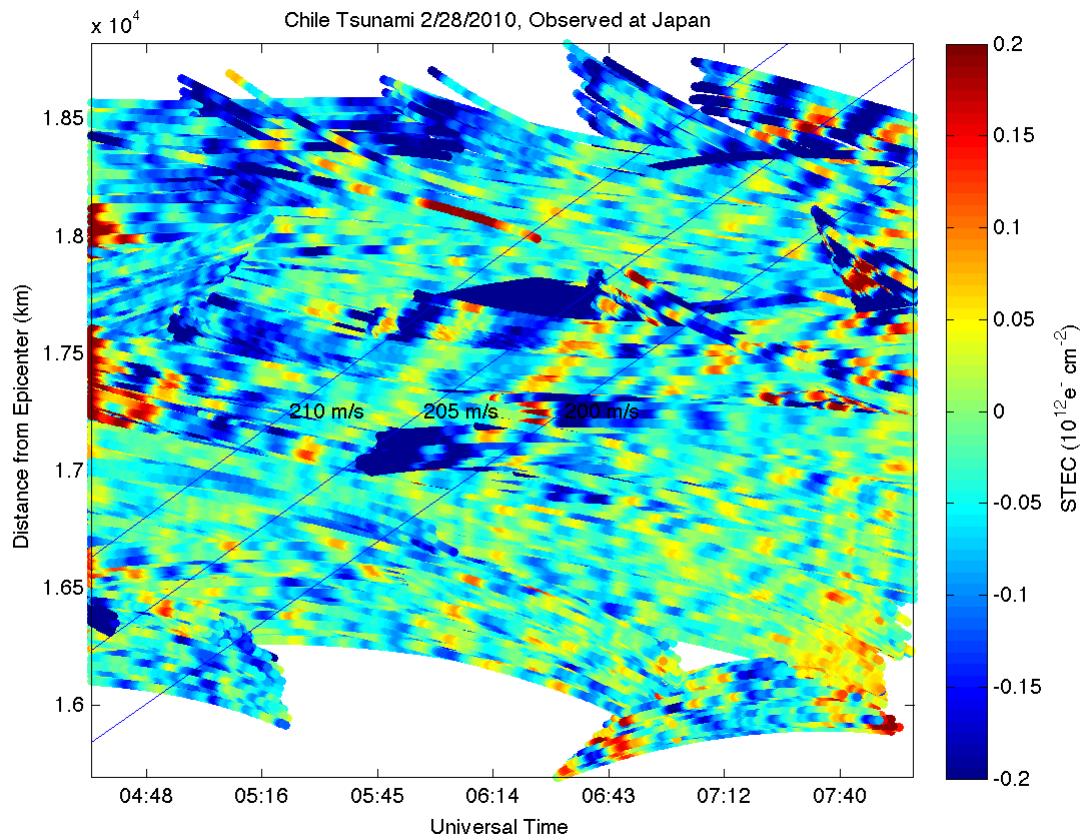


Figure 8. Band-pass filtered slant TEC variation (shown in color) in the region of Japan, plotted as a function of distance from the epicenter of the Chile earthquake of February, 2010, and Universal time. Lines shows a horizontal velocity of ~ 200 m/s, corresponding to typical average tsunami wave speeds.

ionosphere within 15 minutes. Also, there are other sources of TIDs, as discussed earlier, and variations can be generated that have similar wave properties to tsunamis without a tsunami being present. However, given the typically known average horizontal propagation velocity of a tsunami (~ 200 m/s), timing our TEC observations with the expected arrival of the tsunami can help to distinguish those TIDs which are

parameters used to predict the expected runups at coasts that are distant from the source. The Hawaiian islands hold a strategic position at the center of the Pacific Ocean, making the dual-frequency GPS receivers there a prime source of TID observations related to tsunamis originating from elsewhere on the Pacific Rim. If an event generates a significant tsunami somewhere in the Pacific Ocean, it

is likely that the wave will produce a significant signature in the ionosphere that is detectable at Hawaii.

CONCLUSIONS

We have found observational evidence of variations in GPS TEC measurements that are concurrent with the American Samoa tsunami of September 29, 2009 and the Chile tsunami of February 27, 2010. Tsunami-driven internal gravity waves are detected as traveling ionospheric disturbances at Hawaii (for the Samoa and Chile events), and at Japan for the Chile event. Future efforts will apply these research techniques to additional tsunami events to further improve our ability to detect and identify tsunami-driven ionospheric disturbances in GPS TEC data. While the scientific questions regarding the nature of this coupling between the ocean and ionosphere are still being studied, our ongoing research efforts should contribute to assessing the logistical problem of developing a TEC monitoring system that takes advantage of existing real-time networks of GPS receivers, such as the NASA Global Differential GPS System (<http://www.gdgps.net>). Such a system could provide additional information on the inferred amplitude, period, and velocity of a tsunami, based on the observed parameters of the ionospheric internal gravity wave. Such real-time observations could augment the existing tsunami warning system, which currently rely primarily on numerical modeling and buoy observations.

ACKNOWLEDGMENTS

The authors would like to thank Dr. John LaBrecque of NASA Headquarters and the Earth Science and Interior NASA ROSES Grant (NNH07ZDA001N-ESI), which made this research possible. Dr. James Foster of the University of Hawaii provided access to RINEX files from additional GPS receivers on the Big Island of Hawaii. Drs. Edison Gica, Yong Wei, and Vasily Titov of the NOAA Center for Tsunami Research provided access to the MOST model results for the American Samoa (2009) and Chile (2010) tsunami events. Their excellent overview results from these and other tsunami events are available here: http://nctr.pmel.noaa.gov/database_devel.html. Dr. Phillip Stephens in the Ionospheric and Atmospheric Remote Sensing group at JPL also provided useful suggestions and commentary during this research analysis. This research was performed at the Jet Propulsion Laboratory, California Institute of Technology under contract to the National Aeronautics and Space Administration.

REFERENCES

- DART buoy system information available here: http://nctr.pmel.noaa.gov/Dart/dart_home.html
- Artru, J., P. Lognonné, and E. Blanc (2001), Normal modes modelling of post-seismic ionospheric oscillations, *Geophysical Research Letters*, 28, 697–700, 10.1029/2000GL000085.
- Artru, J., V. Ducic, H. Kanamori, P. Lognonné, and M. Murakami (2005), Ionospheric detection of gravity waves induced by tsunamis, *Geophysical Journal International*, 160, 840–848, 10.1111/j.1365-246X.2005.02552.x.
- Calais, E., and J.B. Minster (1995), GPS detection of ionospheric perturbations following the January 17, 1994, Northridge earthquake, *Geophys. Res. Lett.*, 22, 1045-1048, 10.1029/95GL00168.
- Cosgrave, J. (2007) Synthesis Report: Expanded Summary, Joint evaluation of the international response to the Indian Ocean tsunami, published by the Tsunami Evaluation Coalition (TEC), January 2007, 42 p.
- Daniels, F. B. (1952), Acoustical Energy Generated by the Ocean Waves, *Acoustical Society of America Journal*, 24, 83, 10.1121/1.1906855.
- GEONET GPS network information available at: http://terras.gsi.go.jp/gps/geonet_top.html
- Hickey, M. P., G. Schubert, and R. L. Walterscheid (2009), Propagation of tsunami-driven gravity waves into the thermosphere and ionosphere, *J. Geophys. Res.*, 114, A08304, doi:10.1029/2009JA014105.
- Hickey, M. P., G. Schubert, and R. L. Walterscheid (2010), Atmospheric airglow fluctuations due to a tsunami driven gravity wave disturbance, *J. Geophys. Res.*, 115, A06308, doi:10.1029/2009JA014977.
- Hines, C. O. (1972), Gravity Waves in the Atmosphere, *Nature*, 239, 73–78, 10.1038/239073a0.
- Hines, C. O. (1974), *The upper atmosphere in motion*, no. 18 in Geophysical Monograph Series, American Geophysical Union, Washington, D.C.
- Hung, R. J., T. Phan, and R. E. Smith (1978), Observation of gravity waves during the extreme tornado outbreak of 3 April 1974, *Journal of Atmospheric and Terrestrial Physics*, 40, 831–843.
- Kelley, M. C. (2009), *The Earth's Ionosphere: Plasma Physics and Electrodynamics*, *International Geophysics Series*, vol. 96, Elsevier Academic Press.
- Kelley, M. C., R. Livingston, and M. McCready (1985), Large

amplitude thermospheric oscillations induced by an earthquake, *Geophysical Research Letters*, 12, 577–580, 10.1029/GL012i009p00577.

Kelley, M. C. (1997), In situ ionospheric observations of severe weather-related gravity waves and associated small-scale plasma structure, *Journal of Geophysical Research*, 102, 329–336, 10.1029/96JA03033.

Komjathy, A., L. Sparks, B. D. Wilson, and A. J. Mannucci (2005), Automated daily processing of more than 1000 ground-based GPS receivers for studying intense ionospheric storms, *Radio Sci.*, 40, RS6006, doi:10.1029/2005RS003279.

Mai, C.-L., and J.-F. Kiang (2009), Modeling of ionospheric perturbation by 2004 Sumatra tsunami, *Radio Science*, 44, 3011, 10.1029/2008RS004060.

Mannucci, A. J., B. D. Wilson, D. N. Yuan, C. H. Ho, U. J. Lindqwister, and T. F. Runge (1998), A global mapping technique for GPS-derived ionospheric total electron content measurements, *Radio Science*, 33, 565–582, 10.1029/97RS02707.

Meinig, C., S.E. Stalin, A.I. Nakamura, F. González, and H.G. Milburn (2005): Technology Developments in Real-Time Tsunami Measuring, Monitoring and Forecasting. In Oceans 2005 MTS/IEEE, 19–23 September 2005, Washington, D.C. http://nctr.pmel.noaa.gov/Dart/Pdf/mein2836_final.pdf

Nicolls, M. J., M. C. Kelley, A. J. Coster, S. A. González, and J. J. Makela (2004), Imaging the structure of a large-scale TID using ISR and TEC data, *Geophysical Research Letters*, 31, 9812, 10.1029/2004GL019797.

Occhipinti, G., P. Lognonné, E. A. Kherani, and H. Hébert (2006), Three-dimensional waveform modeling of ionospheric signature induced by the 2004 Sumatra tsunami, *Geophysical Research Letters*, 33, L20,104, 10.1029/2006GL026865.

Occhipinti, G., E. A. Kherani, and P. Lognonné (2008), Geomagnetic dependence of ionospheric disturbances induced by tsunamigenic internal gravity waves, *Geophysical Journal International*, 173, 753–765, 10.1111/j.1365-246X.2008.03760.x

Peltier, W. R., and C. O. Hines (1976), On the possible detection of tsunamis by a monitoring of the ionosphere, *Journal of Geophysical Research*, 81, 1995–2000, 10.1029/JC081i012p01995.

Plate Boundary Observatory network information available at: <http://pbweb.unavco.org/>

Richmond, A. D., and S. Matsushita (1975), Thermospheric response to a magnetic substorm, *Journal of Geophysical Research*, 80, 2839–2850, 10.1029/JA080i019p02839.

Tang, A. *et al.* (2010), Learning from Earthquakes: The Mw 8.8 Chile Earthquake of February 27, 2010, Earthquake Engineering Research Institute (EERI), http://www.eeri.org/site/images/eeri_newsletter/2010_pdf/Chil

e10_insert.pdf

Titov, V.V., A.B. Rabinovich, H.O. Mofjeld, R.E. Thomson, and F.I. González (2005): The global reach of the 26 December 2004 Sumatra Tsunami. Science. DOI: 10.1126/science.1114576.

Titov, V.V., and F.I. Gonzalez (1997): [Implementation and testing of the Method of Splitting Tsunami \(MOST\) model](#) NOAA Technical Memorandum ERL PMEL-112, 11 pp. <http://www.pmel.noaa.gov/pubs/PDF/tito1927/tito1927.pdf>

Titov, V.V., and C.E. Synolakis (1997): Extreme inundation flows during the Hokkaido-Nansei-Oki tsunami. *Geophys. Res. Lett.*, 24(11), 1315–1318.

Xiao, Z., S. Xiao, Y. Hao, and D. Zhang (2007), Morphological features of ionospheric response to typhoon, *Journal of Geophysical Research (Space Physics)*, 112, 4304, 10.1029/2006JA011671.

Yeh, K. C., and C. H. Liu (1974), Acoustic-gravity waves in the upper atmosphere, *Reviews of Geophysics*, 12(2), 193–216, 10.1029/RG012i002p00193.

“Search continues, as death toll rises” <http://tvnz.co.nz/national-news/search-continues-death-toll-rises-3045675>. Copyright © 2010, Television New Zealand Limited.

NOAA Center for Tsunami Research Event Page: Samoa September 2009 <http://nctr.pmel.noaa.gov/samoa20090929/>

NOAA National Geophysical Data Center Event Summary for Significant Earthquake, Samoa Islands, 9/29/2009, http://www.ngdc.noaa.gov/nndc/struts/results?EQ_0=4440&t=101650&s=8&d=22.26.13.12&nd=display

NOAA National Geophysical Data Center Event Summary for Significant Earthquake, Chile, 2/27/2010, http://www.ngdc.noaa.gov/nndc/struts/results?EQ_0=4682&t=101650&s=8&d=22.26.13.12&nd=display

Television New Zealand, “Search continues as death rises”. tvnz.co.nz. 2009-10-02. Original URL: <http://tvnz.co.nz/national-news/search-continues-death-toll-rises-3045675>. Archived on 2009-10-04 using webcite: <http://www.webcitation.org/5kHDz9Yyt>.